

Molecular Shape Selectivity through Multiple Carbonyl– π Interactions with Noncrystalline Solid Phase for RP-HPLC

M. Mizanur Rahman, Makoto Takafuji, Hamid R. Ansarian, and Hirotaka Ihara*

Department of Applied Chemistry and Biochemistry, Kumamoto University, 2-39-1 Kurokami, Kumamoto 860-8555, Japan

A new approach for the synthesis of double-alkylated L-glutamide-derived stationary phases to use in RP-HPLC is described. TEM observation of lipid distearylglutamide (DSG) showed the formation of fibrous aggregates in methanol or in chloroform through intermolecular hydrogen bonding among the amide moieties while dibutylglutamide (DBG) cannot aggregate in aqueous or organic media due to its lower order of short alkyl chain. DSG and DBG were covalently bonded to silica via amino-propyl linkages. Lipid membrane analogues (e.g., DSG) attached to the silica surface have been found in noncrystalline and solid states and can form supramolecular assemblies with specific properties based on their highly ordered structures in aqueous and organic media. ^{13}C CP/MAS NMR and suspension (in methanol)-state ^1H NMR, elemental analysis, and DSC measurements were used to characterize Sil-DSG and were compared with the three other octadecyl phases, i.e., monomeric C_{18} , polymeric C_{18} , and silica grafted poly(octadecyl acrylate) Sil-ODA₂₅. The chromatographic behavior of the new RP material was investigated using detailed retention studies of planar and nonplanar polyaromatic hydrocarbons (PAHs) and nonpolar aromatic positional isomers. Aspects of shape selectivity were also evaluated with Standard Reference Materials 869a, Column Selectivity Test Mixture for Liquid Chromatography. Detailed chromatographic study revealed that Sil-DSG showed extremely enhanced molecular shape selectivity compared with the other phases investigated. The higher molecular shape selectivity obtained by Sil-DSG can be explained by a carbonyl π (present in lipid-grafted stationary phases)–benzene π (present in guest PAHs) interaction mechanism, and these interactions are more effective for ordered carbonyl groups.

The evolution of liquid chromatography as a modern analytical technique is due in part to advances made in column technology. Chemical modification of silica packing materials remains a popular approach for achieving novel solute selectivity in high-performance liquid chromatography (HPLC).^{1–4} Most progress

in reversed-phase (RP)-HPLC separation has been achieved due to the introduction of numerous silica-based stationary-phase materials. However, there is still no universal stationary-phase material suited to the specific properties of all possible solutes. Alkylamide phases show interesting chromatographic properties,^{5–8} which are ascribed to the participation in the separation process of different interaction sites, e.g. residual, unreacted silanols, and unreacted amine groups as well as hydrophobic chains with amide groups. In addition, the affinity of these phases to solute molecules differs significantly from that observed for conventional alkyl phases. These advantages have special importance under hydro-organic conditions in binary or ternary mobile phases. Therefore, intermolecular interactions determining elution of solutes of different character on alkylamide phases are interesting from both practical and theoretical points of view. On the other hand, we have proposed⁹ that self-assembled systems such as lipid membrane aggregates can provide a highly ordered microenvironment leading to unique host–guest chemistry exceeding the functions of the original lipid. Earlier we reported about the use of poly(octadecyl acrylate)-grafted silica (Sil-ODA_n), a lipid membrane analogue, as stationary phase for RP-HPLC.^{10,11} Sil-ODA_n showed unique separation behaviors with ordered-to-disordered phase transitions of long alkyl chains. In particular, extremely high selectivity toward polycyclic aromatic hydrocarbons (PAHs) was observed in the ordered (crystalline) state,^{12–15} and the combination of chromophoric diastereomeric reagents yielded better

- (2) Jinno, K.; Yamamoto, K.; Ueda, T.; Nagashima, H.; Itoh, K. *J. Chromatogr.* **1992**, *594*, 105.
- (3) Saito, Y.; Jinno, K.; Pesek, J. J. *Chromatographia* **1994**, *38*, 295.
- (4) Kirkland, J. J.; Glajch, J. L.; Farlee, R. D. *Anal. Chem.* **1989**, *61*, 2.
- (5) Buszewski, B.; Gandzala-Kopciuch, R. M.; Markuszewski, M.; Kalisz, R. *Anal. Chem.* **1997**, *69*, 3277–3284.
- (6) Buszewski, B.; Schmind, J.; Albert, K.; Bayer, E. *J. Chromatogr.* **1991**, *552*, 415.
- (7) Buszewski, B.; Gilpin, R. K.; Jaroniec, M. *J. Chromatogr.* **1994**, *673*, 11.
- (8) Katsuri, P.; Buszewski, B.; Jaroniec, M.; Gilpin, R. K. *J. Chromatogr.* **1994**, *659*, 261.
- (9) Winkle, L. J. V. *Biomembrane Transport*; Academic Press: New York, 1999.
- (10) Disalvo, E. A.; Simon, S. A. *Permeability and Stability of Lipid Bilayers*; CRC Press: Boca Raton, FL, 1995.
- (11) Hirayama, C.; Ihara, H.; Mukai, T. *Macromolecules* **1992**, *25*, 6375.
- (12) Fukumoto, T.; Ihara, H.; Sakaki, S.; Shosenji, H.; Hirayama, C. *J. Chromatogr., A* **1994**, *672*, 237.
- (13) Chowdhury, M. A. J.; Boysen, R. I.; Ihara, H.; Hearn, M. T. W. *J. Phys. Chem. B* **2002**, *106*, 11936.
- (14) Chowdhury, M. A. J.; Ihara, H.; Sagawa, T.; Hirayama, C. *J. Chromatogr., A* **2000**, *877*, 71.
- (15) Ihara, H.; Tanaka, H.; Nagaoka, S.; Sakaki, S.; Hirayama, C. *J. Liq. Chromatogr.* **1996**, *19*, 2967.

* Corresponding author. Tel.: +81 96 342 3662. Fax: +81 96 342 3662. E-mail: ihara@kumamoto-u.ac.jp.

(1) Jinno, K.; Nagoshi, T.; Tanaka, N.; Okamoto, M.; Fetzer, J. C.; Biggs, W. R. *J. Chromatogr.* **1987**, *392*, 75.

selectivity for enantiomers than conventional C₁₈ phases.^{16–18} In general, better separation of PAH isomers can usually be achieved with stationary phases prepared by polymeric surface modification chemistries (compared with monomeric surface modification).^{1,19} Other factors have been shown to influence shape recognition in LC, including stationary-phase bonding density,^{20–22} alkyl-phase chain length,^{23,24} and column temperature,²⁵ and increased shape recognition is due to increased phase order brought on by higher densities, lower temperatures, and longer alkyl-phase chain length. Our detailed investigations showed that the highly ordered structure in Sil-ODA_n induced the orientation of carbonyl groups that work as a π – π interaction source with solute molecules. We have also found that the aligned carbonyl groups are effective for recognition of length and planarity of PAHs through multiple π – π interactions.^{26,27} In this regard, we focused on amino acid derivatives, especially L-glutamic acid-derived lipid membrane analogues. It is well known that the lipophilic L-glutamic acid-derived systems with three amide bonds work as self-assembling materials. Therefore, this new organic system may have potential applications for various fields such as catalysis, sensor technology, materials science, and separation science. We had an attempt to utilize these special amphiphiles in separation science especially in HPLC stationary phases. Considering all these facts, we synthesized two silica-based organic phases (one with short and the other with long alkyl chains) as lipid membrane analogues. Dialkyl L-glutamide-derived amphiphilic lipids form nanotubes,²⁸ nanohelices,^{29–31} and nanofibers³² based on bilayer structures in water and on the fact that intermolecular hydrogen bonding among the amide moieties contributes to self-assembly. Similar self-organization has been realized by lipophilic derivatives of L-glutamide even in organic solvents.^{33–36} The unique properties

exhibited by these self-assemblies can be explained by ordered-to-disordered phase transition, phase separation behavior, and enhancement of the chirality. This paper reports a new approach for the synthesis of a new stationary phase from an L-glutamide-derived lipid membrane analogue based on covalent immobilization. The detailed investigation of chromatographic behavior toward PAHs and the characterization of this newly developed phase will be discussed in this paper.

EXPERIMENTAL SECTION

Materials. The silica-supported L-glutamide-derived stationary phases distearylglutamide (Sil-DSG) and dibutylglutamide (Sil-DBG) were synthesized, characterized, and packed into stainless steel column (250 × 4.6 mm i.d.). A YMC silica (YMC SIL-120-S5 having diameter 4.4 μ m, pore size 12.4 nm, and surface area 339 m² g⁻¹ (YMC-gel, Kyoto, Japan) was used in both cases. Poly(octadecyl acrylate) (Sil-ODA₂₅) uses YMC silica gel, 5- μ m diameter, pore size 12.0 nm, surface area 300 m² g⁻¹ containing 15.7% C in the bonded ligand, was prepared and characterized.¹¹ For spectral (NMR) analysis, we have synthesized both monomeric (13.8% C, 2.7% H, surface coverage by octadecyl moiety was found to be 2.5 μ mol m⁻² or 638 μ mol g⁻¹) and polymeric (23.3% C, 4.3% H with surface coverage 4.9 μ mol m⁻² or 1078 μ mol g⁻¹) C₁₈ grafted silica phases using YMC gel. In contrast, we have used two commercial monomeric and polymeric C₁₈ columns for chromatographic analysis. The monomeric C₁₈ column (Inertsil, ODS 3, column size 250 mm × 4.6 i.d. with particle size 5.5 μ m, pore size 10 nm, and surface area of silica particles 450 m² g⁻¹) was purchased from G. L. Science (Tokyo, Japan). This contains 13.8% C in the bonded octadecyl phase. The polymeric C₁₈ column (Shodex, C18 P, particle size 5 μ m, pore size 10 nm, surface area 300 m² g⁻¹ with end cap of the unreacted silanol group) containing 17.5% C was obtained from Shodex (Tokyo, Japan).

Preparation of L-Glutamide-Derived Lipid Grafted Silica.

The synthesis scheme of lipid distearylglutamide or DSG and the immobilization process of the lipid membrane analogue on to silica is shown in Figure 1. The chemical structures of these compounds were identified by melting point measurements, FT-IR, ¹H NMR, and elemental analysis.

N,N'-Dioctyl-N-benzyloxycarbonyl-L-glutamide (2). N

Benzyloxycarbonyl-L-glutamic acid (L-Glu (Z))³⁷ or **1** (4.0 g, 1.42 × 10⁻² mol), stearylamine (8.6 g, 2.99 × 10⁻² mol), and triethylamine (4.4 g, 4.3 × 10⁻² mol) were dissolved in THF (400 cm³). The solution was cooled to 0 °C, diethylphosphorocyanidate (DEPC) (5.8 g, 3.3 × 10⁻² mol) was added to the solution, and the resultant mixture was stirred for 1 h at this temperature. After being stirred for 1 day at room temperature, the solution was concentrated in vacuo, and the residue was dissolved in 350 cm³ of chloroform. The solution was washed with 10% NaHCO₃, 0.1 M HCl, and water. The solution was dried over Na₂SO₄, concentrated in vacuo, and finally recrystallized from ethanol, which gave white solid powder: yield 10.69 g (96%); mp 133–135 °C; ν_{\max} (KBr)/cm⁻¹ 3296, 3094, 1690, 1644, 1539; ¹H NMR (CDCl₃) δ 0.85–0.90 (t, 6H, CH₃ × 2), 1.2–1.6 (m, 64H, CH₃ (CH₂)₁₆ × 2), 1.85–2.20 (m, 2H, *CHCH₂CH₂C(O)), 2.20–2.45 (m, 2H, CH₂CH₂C(O)NH), 3.20–3.40 (m, 4H, CH₂NHC(O) × 2), 4.00–4.40 (m, 1H, *CH), 4.90–5.20 (s, 2H, CH₂C₆H₅), 7.20–

- (16) Goto, Y.; Nakashima, K.; Mitsuishi, K.; Takafuji, M.; Sakaki, S.; Ihara, H. *Chromatographia* **2002**, *56*, 19.
- (17) Ihara, H.; Takafuji, M.; Sakurai, T.; Tsukamoto, H.; Shundo, A.; Sagawa, T.; Nagaoka, S. *J. Liq. Chromatogr. Relat. Technol.* **2004**, *27* (16), 2559–2569.
- (18) Ihara, H.; Sagawa, T.; Nakashima, K.; Mitsuishi, K.; Goto, Y.; Chowdhury, M. A. J.; Sakaki, S. *Chem. Lett.* **2001**, 1252.
- (19) Sander, L. C.; Wise, S. A. *Anal. Chem.* **1984**, *56*, 504–510.
- (20) Jinno, K.; Tanabe, K.; Saito, Y.; Nagashima, H. *Analyst* **1997**, *122*, 787–791.
- (21) Sentell, K. B.; Dorsey, J. G. *J. Chromatogr.* **1989**, *461*, 193–207.
- (22) Sentell, K. B.; Dorsey, J. G. *Anal. Chem.* **1989**, *61*, 930–934.
- (23) Tanaka, N.; Sakagami, K.; Araki, J.; *J. Chromatogr.* **1978**, *16*, 327–337.
- (24) Sander, L. C.; Wise, S. A. *Anal. Chem.* **1987**, *59*, 2309–2313.
- (25) Sander, L. C.; Wise, S. A. *Anal. Chem.* **1989**, *61*, 1749–1754.
- (26) Ihara, H.; Sagawa, T.; Goto, Y.; Nagaoka, S. *Polymer* **1999**, *40*, 2555.
- (27) Ihara, H.; Goto, Y.; Sakurai, T.; Takafuji, M.; Sagawa, T.; Nagaoka, S. *Chem. Lett.* **2001**, 1252.
- (28) Yamada, K.; Ihara, H.; Ide, T.; Fukumoto, T.; Hirayama, C. *Chem. Lett.* **1984**, 4821.
- (29) Hachisako, H.; Ihara, H.; Hirayama, C.; Yamada, K. *Liq. Cryst.* **1993**, *13*, 307.
- (30) Hachisako, H.; Yamazaki, T.; Ihara, H.; Hirayama, C.; Yamada, K. *J. Chem. Soc., Perkin Trans.* **1994**, *2*, 1671.
- (31) Ihara, H.; Takafuji, M.; Hirayama, C.; O'Brien, D. F. *Langmuir* **1992**, *8*, 1548.
- (32) Ihara, H.; Takafuji, M.; Sakurai, T. *Encyclopedia of Nanoscience and Nanotechnology*; American Science Publishers: Stevenson Ranch, CA, 2004; Vol. 9, pp 473–495.
- (33) Ihara, H.; Hachisako, H.; Hirayama, C.; Yamada, K. *J. Chem. Soc., Chem. Commun.* **1992**, *17*, 1244.
- (34) Ihara, H.; Yoshitake, M.; Takafuji, M.; Yamada, T.; Sagawa, T.; Hirayama, C.; Hachisako, H. *Liq. Cryst.* **1999**, *26*, 1021.
- (35) Ihara, H.; Sakurai, T.; Yamada, T.; Takafuji, M.; Sagawa, T.; Hachisako, H. *Langmuir* **2002**, *18*, 7120.
- (36) Fukumoto, T.; Ihara, H.; Sakaki, S.; Shosenji, H.; Hirayama, C. *J. Chromatogr.* **1994**, *672*, 237.

(37) Bergmann, M.; Lervas, Z. *Ber. Dtsch. Chem. Ges.* **1932**, *65*, 1192.

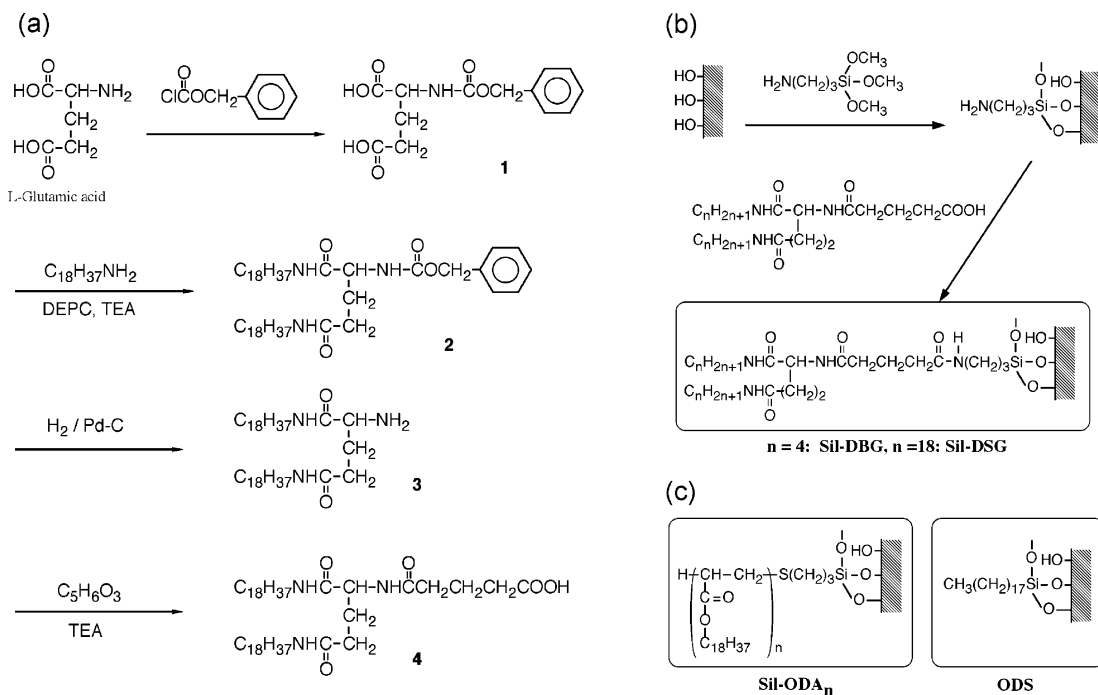


Figure 1. Reaction schemes for the synthesis of (a) diostearyl L-glutamide (DSG) lipid membrane analogue, (b) immobilization of lipid on to silica gel, and (c) and (d) structure of Sil-DBG and Sil-ODA_n.

7.45 (s, 5H, C_6H_5). Elemental analysis (Anal. Found: H, 11.32; C, 74.80; N, 5.23 Cal. For $C_{49}H_{90}N_3O_4$: H, 11.43; C, 75.04; N, 5.35%).

***N,N'*-Dioctadecyl-L-glutamide (3).** *N,N'*-Dioctyl-*N*-benzoyloxycarbonyl-L-glutamide or **2** (3.5 g, 5.5×10^{-3} mol) was dissolved in 300 cm³ of ethanol and THF (50:50 by volume) with heating, and Pd carbon black (1 g) was added to the solution. H_2 gas was bubbled slowly into the solution for 10 h at 60 °C. Pd carbon black was removed by filtration. The solution was concentrated, recrystallized from ethanol, and dried in vacuo to give a white solid powder: yield 2.15 g (85%); ν_{max} (KBr)/cm⁻¹ 3318, 2962, 2934, 2874, 1647, 1553; ¹H NMR ($CDCl_3$) δ 0.85–0.90 (t, 6H, $CH_3 \times 2$), 1.2–1.6 (m, 64H, CH_2 (CH_2)₁₆ $\times 2$), 1.85–1.98 (m, 2H, *CHCH₂-CH₂C(O)), 2.30–2.45 (m, 2H, CH₂CH₂C(O)NH), 3.10–3.30 (m, 4H, CH₂NHC(O) $\times 2$), 3.6–3.85 (m, 1H, *CH). Elemental analysis (Anal. Found: H, 12.63; C, 75.39; N, 6.48 Cal. For $C_{41}H_{83}N_3O_2$: H, 12.8; C, 75.7; N, 6.46%).

***N,N'*-Dioctadecyl-*N*^a-[4-carboxybutanoyl]-L-glutamide (4).** *N,N'*-dioctadecyl-L-glutamide or **3** (3 g, 4.78×10^{-3} mol) and triethylamine (0.90 cm³, 6.45×10^{-3} mol) were dissolved in 300 cm³ of chloroform and stirred with cooling. Glutaric anhydride (0.90 g, 7.9×10^{-3} mol) was added to the solution. After being stirred for 4 h at room temperature, the solution was concentrated in vacuo. The residue was recrystallized from ethanol and dried in vacuo, which gives a white solid powder: yield 87%; mp 128–130 °C; ν_{max} (KBr)/cm⁻¹ 3288, 2917, 2849, 1730, 1637, 1533; ¹H NMR ($CDCl_3$) δ 0.78–0.98 (m, 6H, $CH_3 \times 2$), 1.2–1.6 [m, 64 H, (CH_2)₁₆ $\times 2$], 2.0–2.47 [m, 6H, CH₂C(=O)NH $\times 2$, CH₂C(=O)], 3.2–3.50 [m, 4H, CH₂NHC(=O) $\times 2$], 4.10–4.4 (m, 1H, *CH). Elemental analysis: (Anal. Found: H, 11.63; C, 71.99; N, 5.52 Cal. For $C_{45}H_{89}N_3O_5$: H, 11.7; C, 72.3; N, 5.5%).

DBG was synthesized and characterized according to the procedure described above.

Immobilization of Lipid Membrane Analogue (DSG) on to Silica. (3-Aminopropyl)trimethoxysilane (APS) grafted silica (**5**) (Sil-APS) was prepared by refluxing porous silica gel (3.0 g) and 1.5 cm³ of APS in toluene for 20 h. After successive washing with toluene, ethanol, and diethyl ether, the particles were dried in vacuo. The dried particles were characterized by elemental analysis (H, 2.2; C, 8.4; N, 2.6%). Sil-APS was then coupled with lipid **4**. Sil-APS or **5** (3.0 g) and lipid **4** (3.0 g, 3.92×10^{-3} mol) were taken in 100 cm³ of dry THF and stirred. DEPC (1.5 g, 9.6×10^{-3} mol) and TEA (1.1 g, 10.6×10^{-3} mol) were added to the solution and stirred at 60 °C. After being stirred for 1 day, the grafted particles were washed with hot THF and hot chloroform several times to remove the unreacted lipid molecule and dried in vacuo. The phase transition behavior of lipid (solid or in suspension with methanol or ethanol) and the stationary phases (both as solid powder and in suspension of methanol and ethanol) were done by differential scanning calorimetry (DSC) measurement.

Transmission Electron Microscopy (TEM). Transmission electron micrographs were recorded by using a JEOL 2000FX. The samples were spotted on carbon-coated copper grids (200 Å). After excess of the samples was removed by a tissue paper and air-dried, they were stained with 2 wt % molybdate.

Differential Scanning Calorimetry (DSC). DSC was carried out using EXTRA 6000 with DSC6200 from Seiko Instruments Inc.

Spectroscopic Measurements. Conformational structures and the mobility of alkyl chain of the stationary phase were determined by measuring suspension-state ¹H NMR and solid ¹³C CP/MAS NMR spectra. NMR spectra was measured by Varian Unity-Inova AS400 at a static magnetic field of 9.4 T using nanoprobe GHX for suspension-state NMR and solid probe for CP/MAS NMR as spin rate of 2000–3500 Hz for suspension-state NMR and 4000–

4500 Hz for solid-state NMR. The samples for suspension-state ^1H NMR were made by using 10 mg of each stationary phase in 100 μL of CD_3OD including 0.03% tetramethylsilane and 0.05% hexamethylsilane. All samples were prepared at the same time using one single ampule of CD_3OD . Hexamethylsilane was added to work as a reference of intensity, but protons of CD_3OD proved better for this purpose. ^1H NMR spectra were measured at 20–50 $^\circ\text{C}$ at every 5 $^\circ\text{C}$ interval using a GHX Varian AS400 nanoprobe. The parameters used for measurement were delay time 1.5 s, pulse width 2.2, transient numbers 32, and spectral width 6000 Hz. Water was suppressed using a presaturation pulse sequence with saturation delay of 1.5 s and saturation power of 2 db. For assigning peaks, after determination of pulse width of 90 $^\circ$ simple RELAY COSY (correlation spectroscopy test) was done and the chemical shifts of the terminal methyl and methylene proton of alkyl chain were determined. For solid-state ^{13}C CP/MAS, the NMR measuring parameters are spectral width 50 000 Hz, proton pulse width $\text{PW } 90 = 11.6 \mu\text{s}$, contact time for cross polarization 5 ms, and delay before acquisition was 2 s. High-power proton decoupling of 63 db with fine attenuation of dipole $r = 2500$ was used only during detection periods.

Chromatography. The chromatographic system consists of a Gulliver PU-980 intelligent HPLC pump with a Rheodyne sample injector having 20- μL loop. A Jasco multiwavelength UV detector MD 2010 plus was used. The column temperature was maintained by using a column jacket with a circulator having a heating and a cooling system. A personal computer connected to the detector with Jasco-Borwin (Ver 1.5) software was used for system control and data analysis. As the sensitivity of UV detector is high, 5 μL of sample solution was used for each injection. To avoid overloading effects, special attention was given in this study to the selection of optimum experimental conditions. Separations were performed using HPLC grade methanol and water mixture (90:10) or ethanol as mobile phase at a flow rate 1.00 mL min^{-1} . The retention factor (k) measurement was done under isocratic elution conditions. The separation factor (α) is the ratio of the retention factor of two solutes that are being analyzed. The chromatography was done under isocratic elution conditions. The retention time of D_2O was used as the void volume (t_0) marker (The absorption for D_2O was measured at 400 nm, which actually considered as injection shock). All data points were derived from at least triplicate measurements; with retention time (t_R) value varying $\pm 1\%$. Water/1-octanol partition coefficient ($\log P$) was measured by the retention studies with octadecylated silica, C_{18} (monomeric) (Inertsil ODS, i.d. 250 mm \times 4.6 mm, GL Science, Tokyo, Japan): $\log P = 3.579 + 4.207 \log k$ ($r = 0.999\ 997$).¹⁶

RESULTS AND DISCUSSION

Brief Description on Dialkyl-L-glutamide-Derived Lipid Bonded Stationary-Phase Synthesis. Double-alkylated L-glutamide-derived derivatives DSG and DBG were synthesized from *N*-benzyloxycarbonyl-L-glutamic acid through alkylation, debenzyl-oxycarbonylation, and ring-opening reaction with glutaric anhydride. The lipid DSG containing three amide groups per molecule formed a gel in organic solvents (e.g., benzene, toluene, chloroform, and THF), which exhibited a thermoreversible gel-to-sol phase transition behavior with concentration as low as 2 mmol L^{-1} . In our previous studies, we have reported that dialkyl L-glutamide-derived lipid with long alkyl chain formed highly

Table 1. Elemental Analysis Data of Sil-APS and Lipid-Grafted Stationary Phases

	% C	% H	% N	C/N
Sil-APS	8.40	2.20	2.70	3.11
Sil-DSG	20.1	3.10	2.98	6.74
Sil-DBG	13.5	2.58	2.69	5.10

oriented structures with chiral arrangements below T_c and that the molecular assembly is brought about by complementary hydrogen bonds between the neighboring molecules in the lipid.^{38–41} On the other hand, DBG cannot form gel in aqueous or in organic media even at higher concentrations (100 mmol L^{-1}) due to the lower ordering ability of the short alkyl chain. TEM observation of lipid DSG and DBG in methanol, chloroform, and toluene showed that DSG forms fibrous aggregates whereas DBG cannot form aggregates in aqueous or in organic solvents. The aggregation of the lipid molecule in organic solvents can make the carbonyl group in a highly ordered state by forming hydrogen bonding between the amide moieties

The lipid molecules were immobilized onto APS grafted silica (Sil-APS) by covalent linkages (amide bond via aminopropylsilica as shown in Figure 1) using DEPC. The elemental analysis results for Sil-APS, Sil-DSG, and Sil-DBG are shown in Table 1. The C/N value of Sil-APS is 3.11, which indicates that almost all of the methoxy groups of APS were consumed for silanation to silica, for cross-linking, or for both. The surface coverage with APS was calculated from the carbon percentage (C%) of Sil-APS to be 7.84 $\mu\text{mol m}^{-2}$. The percentage of carbon in Sil-DSG was found to increase from 8.41 to 20.1 after the grafting process. Surface coverage and alkyl chain densities of different stationary phases were calculated by using the equations given below, these equations were also mentioned in our recent paper.⁴²

The molar amount of organic phase per 1 g silica (M) can be calculated as

$$M (\mu\text{mol g}^{-1}) = 10^6 (P_C/100)/12n \quad (1)$$

where P_C is the percentage of carbon element according to elemental analysis and n is the number of carbons present in the grafted organic phases.

The weight percentage of the grafted phase (P_w) in each case can be calculated as

$$P_w = m \times 10^{-4} M (n/n_1) \quad (2)$$

where m is the molecular mass and n_1 is the number of carbon in each molecule of the organic phases grafted onto silica surface.

(38) Ihara, H.; Shudo, K.; Hirayama, C.; Hachisako, H.; Yamada, K. *Liq. Cryst.* **1996**, *20*, 807.

(39) Hachisako, H.; Ihara, H.; Kamiya, T.; Hirayama, C.; Yamada, K. *J. Chem. Soc., Chem. Commun.* **1997**, 19.

(40) Ihara, H.; Yushitake, M.; Takafuji, M.; Yamada, T.; Sagawa, T.; Hirayama, C.; Hachisako, H. *Liq. Cryst.* **1999**, *26*, 1021.

(41) Takafuji, M.; Ihara, H.; Hirayama, C.; Hachisako, H.; Yamada, K. *Liq. Cryst.* **1995**, *18*, 97.

(42) Ansarian, H. R.; Derakshan, M.; Rahman, M. M.; Sakurai, T.; Takafuji, M.; Taniguchi, I.; Ihara, H. *Anal. Chim. Acta* **2005**, *547*, 179–187.

Furthermore, the surface coverage (N) can be calculated as

$$N (\mu\text{mol m}^{-2}) = M / \{S[(100 - P_w)/100]\} = 10^6 P_c / [12nS(100 - P_w)] \quad (3)$$

where S is surface area of 1.00 g of nonmodified silica.

The alkyl chain density can be calculated as

$$D (\mu\text{mol m}^{-2}) = Nf \quad (4)$$

where the factor (f) indicate the number of alkyl chain present in the grafted molecule. For C_{18} , it is considered as 1, for SiI-ODA_n , f is degree of polymerization (in this case $f = 25$), and for L-glutamide-derived dialkyl stationary phase $f = 2$.

It is obvious that only monomeric C_{18} ($1.72 \mu\text{mol m}^{-2}$) showed a lower alkyl chain density than SiI-DSG ($2.13 \mu\text{mol m}^{-2}$). The suspension of SiI-DSG and SiI-DBG in methanol or in ethanol showed no phase transition in thermal analysis using DSC. We have reported previous work that significant phase transition of poly(octadecyl acrylate) was observed even after a terminal group was grafted onto the silica surface (SiI-ODA_n).^{13,14} This is due to a small perturbation on the silica surface because only one side of the polymer main chain is chemically bonded, allowing the polymer side chain to remain flexible. For SiI-DSG and SiI-DBG , the lipid molecule was directly connected to the silica surface, and thus, the mobility is strongly restricted.

Suspension-State ^1H NMR Spectroscopic Measurements.

Although half-height width and transverse relaxation time (T_2) are important indicators of molecular mobility of phases, these variables were not found to be dependable in our study because the NMR intensity of methylene groups was too small to obtain a reliable measurement. The NMR peak is a superimposition of several methylene groups with different relaxation times that flaws the relation between the measured T_2 and the mobility on a theoretical basis. Therefore, we turned to the rather new but simple approach of determining the percentages of octadecyl moieties in liquid-type mobility in each case. The form of motionally averaged Hamiltonian depends very strongly on the type and the time scale of molecular motion and, hence, on the phase of the matter. In liquid- or suspension-state NMR, only those molecules or parts of molecules with very fast rotational motions are detectable. Motion must be in such a fast range that it can average out dipolar coupling and chemical shift anisotropy until related NMR peaks become narrow enough to be detected. The suspension-state ^1H NMR of four different stationary phases were measured from 20 to 50 °C. Neither half-height width (line width) of methylene groups nor spin-spin relaxation time (T_2) showed any significant change with temperature (20–50 °C). We observed that intensity of the NMR peaks representing terminal methyl and methylene groups of octadecyl moieties increased significantly in SiI-ODA_{25} . In monomeric C_{18} , the intensity of the NMR peaks representing terminal methyl and methylene groups increased slightly, but in polymeric C_{18} , only the peak of methylene groups was detectable when a very high vertical scale was used for graphical presentation. On the other hand, SiI-DSG also showed similar increases, but lower than those for monomeric C_{18} .

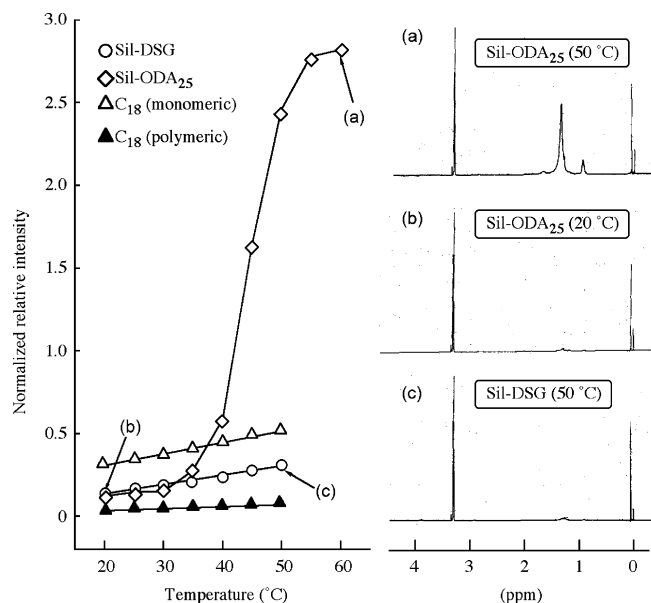


Figure 2. Temperature dependencies of normalized relative ^1H NMR intensities of methylene groups of different stationary phases in (a), suspension-state ^1H NMR spectra of SiI-ODA_{25} at 20 °C in (b), 50 °C in (c), and ^1H NMR spectra of SiI-DSG at 50 °C in (d).

Intensities, to be comparable among all phases at various temperatures, are weighted according to the following formula.

$$I (\mu\text{mol}^{-1}) = (I_m/I_D) / (4 \times 10^{-3}M) = 250 [I_m/(I_D M)]$$

I , the normalized intensity (relative intensity of NMR signal per $1 \mu\text{mol}$ of octadecyl moiety) is as shown in Figure 2. I_m is the underpeak area of the methylene peak, I_D is the intensity of the few protons belonging to methanol, and M is the amount of grafted organic molecule per 1 g of modified silica. Normalized intensity of ^1H NMR peak of methylene groups on SiI-ODA_{25} begins to increase distinctly at ~ 35 °C, but no similar trends are observed for SiI-DSG and C_{18} phases. This corresponds to the crystalline-to-isotropic phase transition of side alkyl chain of SiI-ODA_{25} . The mobility of methylene groups was strongly restricted in crystalline state. The order of normalized intensity is polymeric $C_{18} < \text{SiI-ODA}_{25} < \text{SiI-DSG} < \text{monomeric ODS}$ at 20 °C, but above the phase transition temperature of SiI-ODA_{25} the order changed to polymeric $C_{18} < \text{SiI-DSG} < \text{monomeric ODS} < \text{SiI-ODA}_{25}$. Compared with SiI-ODA_{25} , the normalized intensities of other silica-supported polymers increased slightly and showed no bending point in the temperature range from 20 to 50 °C. These results indicate that the organic phases on the silica surface of all stationary phases are in a solid state at room temperature, but the mobility of methylene groups in organic phase is different for each stationary phase. Since only SiI-ODA_{25} shows remarkable enhancement of mobility, it is assumed that direct immobilization does not allow long alkyl chain-containing molecules to exist in liquid state.

^{13}C CP/MAS NMR Spectroscopic Measurements. Solid-state NMR spectroscopy is a powerful tool for evaluation of the chemical composition and conformational properties of chemically modified surfaces. ^{13}C CP/MAS NMR spectra were acquired for SiI-DSG , SiI-ODA_{25} , and monomeric and polymeric C_{18} phases. The

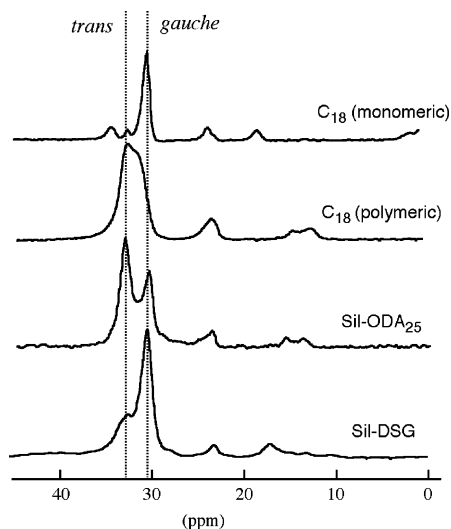


Figure 3. Typical ^{13}C CP/MAS NMR spectra of different stationary phases at 20 °C.

intense signal at ~ 30 ppm is attributed to the methylene carbons with long alkyl chains in the bonded organic phase. The signals of aminopropyl spacer appear at 10, 17, and 41 ppm. The signal at 176 ppm results as a consequence of the peptide bonds among the glutamide moiety. To investigate the conformations of the n -alkyl units in the grafted chain, ^{13}C CP/MAS NMR spectra were recorded. Under the conditions of magic angle spinning and dipolar coupling of protons, the chemical shift of ^{13}C NMR spectrum depended largely on the conformation of alkyl chains. ^{13}C CP/MAS NMR spectra of the octadecyl-containing phases used in this study are compared in Figure 3. It is well known that the ^{13}C signal for $(\text{CH}_2)_n$ carbon atoms is observed at two resonances, one at 32.6 due to trans conformation, indicating rigid and ordered chains, and the other at 30.0 ppm due to gauche conformation, characterizing mobile and amorphous regions.^{43–45} The ^{13}C CP/MAS NMR spectra for Sil-DSG at room temperature showed domination of gauche ($\delta = 30.4$ ppm) and a low-field shoulder indicating a trans ($\delta = 32.46$ ppm) that remains almost the same even at temperatures as high as 50 °C. On the other hand, Sil-ODA₂₅ demonstrated two well-resolved peaks, trans ($\delta = 32.96$ ppm) and gauche ($\delta = 29.98$ ppm) conformation. Monomeric C₁₈ showed almost only gauche ($\delta = 30.4$) and polymeric C₁₈ showed predominantly trans ($\delta = 32.84$ ppm) with an upfield shoulder indicating gauche conformation. At a temperature of 50 °C, polymeric C₁₈ shows predominantly gauche ($\delta = 31.5$ ppm) conformation with a low-field shoulder indicating trans. The chemical shift of gauche conformation in the case of polymeric C₁₈ (31.5 ppm) is still considerably higher than Sil-DSG (30.16 ppm) and Sil-ODA₂₅ (29.98 ppm). Polymeric C₁₈ has a gauche peak 1.4 ppm higher than Sil-DSG and 1.52 ppm higher than Sil-ODA₂₅. Interestingly, we see two peaks rather than one around the chemical shift of 12–14 ppm for polymeric C₁₈ and Sil-ODA₂₅. According to Pursch et al.,⁴⁶ in polymeric C₁₈, these two peaks are assigned as C1 (carbon attached to the silica

surface) at resonance 14.1 ppm and C18 (carbon present in the terminal methyl group). A similar phenomenon is also observed for Sil-ODA₂₅, while in Sil-DSG there is no peak at around 12–14 ppm. This difference may happen due to the differences in microenvironment of these two phases and also from conformational effect.

From detailed spectroscopic as well as DSC measurement, it was found that the organic phase (lipid) in Sil-DSG remained solid and in a noncrystalline state even at higher temperatures unlike Sil-ODA₂₅ and polymeric C₁₈ phases.

Selectivity for Alkylbenzenes. It is known that conventional C₁₈ or alkyl phases can recognize the hydrophobicity of elutes and this hydrophobicity is measured by the methylene activity of the stationary phases. This reflects the possibility of the phase being able to separate two molecules that differ only in methylene groups, e.g., amylbenzene and butylbenzene or ethylbenzene and toluene. The retention mode as well as the extent of hydrophobic interaction between the elutes and the packing materials in HPLC can be determined by retention studies of alkylbenzenes as elutes.^{47–50} Other tests use the retention factors of chrysene,⁵¹ toluene,⁵² or acenaphthacene.²³ Figure 4 shows the relationship between $\log k$ and $\log P$ for Sil-DSG, Sil-DBG, monomeric C₁₈, and Sil-ODA₂₅ phases. It is also observed that the retention mode of Sil-DSG and Sil-DBG showed a reversed-phase mode to that of conventional C₁₈ phase. As shown in Figure 4, Sil-DSG showed extremely lowered retention of alkylbenzenes as compared with C₁₈ and even lower than that of Sil-ODA₂₅. All the samples (both alkylbenzene and PAHs) showed least retention on Sil-DBG although a higher amount of water was used (30%) in the mobile phase than others (10%). It was also observed that $\log k$ and $\log P$ plots of alkylbenzenes and PAHs in C₁₈ were parallel and almost coincided with each other. This happened because monomeric C₁₈ can recognize only the hydrophobicity of elutes. It has been found that Sil-DSG showed higher retention for PAHs compared to its values for alkylbenzenes. For instance, the $\log P$ of naphthacene (5.71) is much smaller than dodecylbenzene (8.43), but the $\log k$ value of naphthacene (0.86) is higher than dodecylbenzene (0.74). The increase of $\log k$ for PAHs was accompanied by selectivity enhancement. For example, $\alpha_{\text{Naphthacene/Triphenylene}} = 3.36$ for Sil-DSG whereas monomeric C₁₈ yielded $\alpha_{\text{Naphthacene/Triphenylene}} = 1.22$. These results indicate that the Sil-DSG phase provides specific interactive sites for PAHs like Sil-ODA_n which recognizes aromaticity through carbonyl- π interaction.^{16,53} The detailed chromatographic behavior with separation mechanism will be discussed in the following section.

Selectivity toward PAHs. Several size and shape parameters for PAHs were introduced for systematic investigations on

(43) Pursch, M.; Strohschein, S.; Handel, H.; Albert, K. *Anal. Chem.* **1996**, *68*, 386–393.

(44) Tonelli, A. E.; Schiling, F. C.; Bovey, F. A. *J. Am. Chem. Soc.* **1984**, *106*, 1157.

(45) Pursch, M.; Sander, L. C.; Albert, K. *Anal. Chem.* **1996**, *68*, 4107–4113.

(46) Pursch, M.; Brindle, R.; Ellvanger, A.; Sander, L. C.; Bell, C. M.; Handel, H.; Albert, K. *Solid State Nucl. Magn. Reson.* **1997**, *9*, 191.

(47) Shundo, A.; Sakurai, T.; Takafuji, M.; Nagaoka, S.; Ihara, H. *J. Chromatogr., A* **2005**, *1073*, 169–174.

(48) Ihara, H.; Dong, W.; Mimaki, T.; Nishihara, M.; Sakurai, T.; Takafuji, M.; Nagaoka, S. *J. Liq. Chromatogr.* **2003**, *26*, 2473.

(49) Claessens, H. A.; Van Straten, M. A.; Cramers, C. A.; Jezierska, M.; Buszewski, B. *J. Chromatogr., A* **1998**, *826*, 135.

(50) Sadek, P. C.; Carr, P. W. *J. Chromatogr. Sci.* **1983**, *21*, 314.

(51) Jost, W.; Gasteier, R.; Schwinn, G.; Tueylue, M.; Majors, R. E. *Int. Lab.* **1990**, (May), 46.

(52) Neue, U. D.; Phillips, D. J.; Walter, T. H.; Caparella, M.; Alden, B.; Fisk, R. P. *LC-GC Int.* **1995**, *8*, 26.

(53) Sakaki, S.; Kato, K.; Miyazaki, T.; Ohkubo, K.; Ihara, H.; Hirayama, C. *J. Chem. Soc., Faraday Trans 2.* **1993**, *9*, 659.

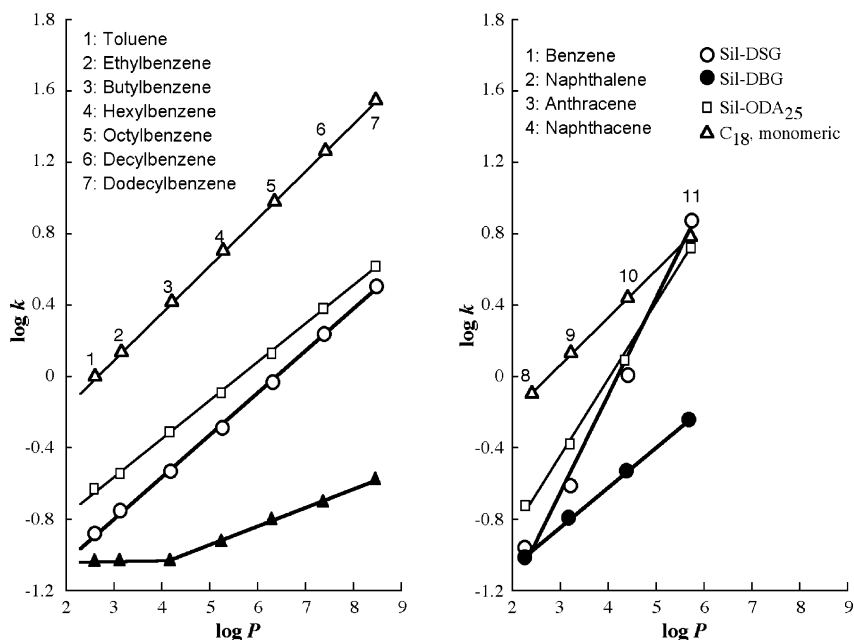


Figure 4. Relationships between $\log k$ and $\log P$ of different stationary phases. Mobile phase: methanol–water (90/10 v/v) for monomeric C_{18} , Sil-ODA₂₅, and for Sil-DSG, methanol–water (70/30 v/v) was used for Sil-DBG. Column temperature: 30 °C. Elutes: 1, benzene; 2, naphthalene; 3, anthracene; 4, naphthacene; 5, toluene; 6–11, ethyl-, butyl-, hexyl-, octyl-, decyl-, and dodecylbenzene.

retention behavior. The F number is a molecular size descriptor proposed by Hurtubise et al.,⁵⁴ which is defined as follows: $F = (\text{number of double bonds}) + (\text{number of primary and secondary carbons}) - 0.5(\text{number of nonaromatic rings})$. The selectivity for the two-dimensional shape has been further studied with a molecular shape descriptor, length-to-breadth (L/B) ratio. The parameter was proposed by Wise et al.⁵⁵ and Kaliszán et al.⁵⁶ and has been defined as the length-to-breadth ratio of the two-dimensional shape of a molecule, and it quantitatively classifies “rodlike” molecules and “squarelike” molecules. The combination of these size and shape parameters, F and L/B, has been successfully introduced for the characterization of C_{18} phases.⁵⁷ The detailed retention data of PAHs on different stationary phases is given in Table 3. To evaluate the planarity recognition capability of C_{18} phases, Tanaka et al.^{58,59} and Jinno et al.^{60,61} introduced the selectivity for two solutes, *o*-terphenyl ($F = 9$, L/B = 1.11) and triphenylene ($F = 9$, L/B = 1.12). Other sample sets (phenanthrene/*cis*-stilbene, flourene/diphenylmethane) were also used to assess the planarity recognition ability of unknown stationary phase.⁶² We observed that Sil-DSG ($\alpha_{\text{triphenylene}/o\text{-terphenyl}} = 5.70$) showed extremely enhanced molecular planarity recognition

Table 2. Alkyl Chain Densities of Different Phases

	surface area of silica $\text{m}^2 \text{g}^{-1}$	% C	alkyl chain density $\mu\text{mol m}^{-2}$
C_{18} , monomeric	450	13.8	1.72
C_{18}^a , monomeric	300	13.8	2.50
C_{18} , polymeric	300	17.5	3.40
C_{18}^a , polymeric	300	23.3	4.90
Sil-ODA ₂₅	300	15.7	2.61
Sil-DBG	339	5.1	1.53
Sil-DSG	339	11.7	2.13

^a C_{18} phases used for NMR measurements.

ability compared to other phases studied; for instance, monomeric C_{18} demonstrated $\alpha_{\text{triphenylene}/o\text{-terphenyl}} = 1.5$, polymeric C_{18} $\alpha_{\text{triphenylene}/o\text{-terphenyl}} = 3.0$, Sil-ODA₂₅ $\alpha_{\text{triphenylene}/o\text{-terphenyl}} = 4.5$, and Sil-DBG $\alpha_{\text{triphenylene}/o\text{-terphenyl}} = 2.6$. Planar and nonplanar solutes retention have also been investigated for PAHs with similar L/B values but dissimilar planarity.^{20,63} In this model, a stationary phase is represented as consisting of a number of slots into which a solute molecule can penetrate during retention. For slots of finite size, planar solutes penetrate more slots and will be retained in preference to nonplanar solutes, and long narrow molecules with higher L/B ratio will be retained in preference to square molecules. Naphthacene (L/B = 1.89) long narrow molecules with large length eluted later in Sil-DSG than pyrene (L/B = 1.27) square-shaped molecules. Retention of coronene (a planar PAH with L/B = 1.00) and phenanthro[34-*c*]phenanthrene (PhPh) a nonplanar PAH with L/B = 1.07 was also studied. The k ratio for coronene to PhPh is 17.27 for Sil-DSG, indicating that significantly greater planar/nonplanar shape discrimination is possible by Sil-DSG. This distinction is also valid for linear and nonlinear molecules, i.e., naphthacene and chrysene in Sil-DSG. We have

- (54) Schborn, J. F.; Hurtubise, R. J.; Silver, H. F. *Anal. Chem.* **1983**, *49*, 2253–2260.
 (55) Wise, S. A.; Bonnet, W. J.; Guenther, F. R.; May, W. E. *J. Chromatogr. Sci.* **1981**, *19*, 248–255.
 (56) Kaliszán, R.; Lamparczyk, H.; W. J.; Guenther, F. R.; May, W. E. *J. Chromatogr. Sci.* **1978**, *16*, 246–248.
 (57) Jinno, K., Ed. *Chromatographic Separations Based on Molecular Recognition*; Wiley-VCH: New York, 1997; p 65.
 (58) Tanaka, N.; Tokuda, Y.; Iwaguchi, K.; Araki, J. *J. Chromatogr.* **1982**, *239*, 761–771.
 (59) Kimata, K.; Iwaguchi, K.; Onshi, S.; Jinno, K. Eksteen, R.; Hosoya, K.; Araki, M.; Tanaka, N. *J. Chromatogr. Sci.* **1989**, *27*, 721–728.
 (60) Jinno, K.; Yamamoto, K.; Nagashima, H.; Ueda, T.; Itoh, K. *J. Chromatogr.* **1990**, *517*, 193–207.
 (61) Jinno, K.; Mae, H. *J. High Resolut. Chromatogr.* **1990**, *13*, 512–515.
 (62) Jinno, K.; Tanabe, K.; Saito, Y.; Nagashima, H. *Analyst* **1997**, *122*, 787–791.

- (63) Wegmann, J.; Albert, K.; Pursch, M.; Sander, L. C. *Anal. Chem.* **2001**, *73*, 1814–20.

Table 3. Retention and Separation Factors of PAHs for Different Stationary Phases^a

	MW	L/B	^x C ₁₈ (mon)		^x C ₁₈ (polym)		^x Sil-ODA ₂₅		^y Sil-DBG		^x Sil-DSG	
			<i>k</i>	<i>α</i>	<i>k</i>	<i>α</i>	<i>k</i>	<i>α</i>	<i>k</i>	<i>α</i>	<i>k</i>	<i>α</i>
¹ Benzene	78	1.099	0.81	1.80	0.56	2.0	0.21	2.14	0.10	4.3	0.11	2.55
¹ Naphthalene	128	1.238	1.46		1.12		0.45		0.43		0.28	
¹ Diphenylenemethane	166	1.520	1.78	1.23	1.19	1.6	0.38	1.90	1.06	1.43	0.61	2.07
¹ Fluorene	166	1.520	2.19		1.90		0.72		1.50		1.26	
¹ Phenanthrene	178	1.463	2.79	1.08	2.52	1.2	1.00	1.22	0.89	1.02	0.84	1.31
¹ Anthracene	178	1.566	3.00		3.00		1.22		0.91		1.10	
¹ Pyrene	202	1.257	4.42	1.23	4.56	1.29	1.90	1.47	1.43	1.35	1.68	1.75
¹ Triphenylene	228	1.119	5.43		5.89		2.80		1.92		2.94	
¹ Benzo-a-anthracene	228	1.599	5.84	1.08	6.72	1.15	3.70	1.32	2.13	1.10	3.94	1.34
¹ Chrysene	228	1.734	5.84	1.08	6.90	1.17	4.00	1.43	2.23	1.16	4.86	1.65
¹ Naphthacene	228	1.896	6.90	1.27	9.37	1.60	7.20	3.08	2.31	1.20	11.3	3.85
² Benz[e]acenaphthylene	252	1.387	0.90	1.02	1.11	1.08	1.15	1.13	3.42	0.91	1.22	1.22
² Benz[k]fluoranthene	252	1.474	0.88		1.20		1.30		3.12		1.48	
² Benzo-e-pyrene	252	1.118	0.71	1.02	1.24	1.07	0.45	1.08	2.62	1.02	1.46	1.21
² Perylene	252	1.276	0.72	1.07	1.32	1.26	0.48	1.27	2.66	1.05	1.76	1.31
² Benzo-a-pyrene	252	1.493	0.76		1.56		0.57		2.75		1.90	
² Dibenzo[a,c]anthracene	278	1.238	0.72	1.04	1.31	1.12	0.57	1.26	3.53	1.05	2.02	1.87
² Dibenzo[a,h]anthracene	278	1.822	0.75	1.88	1.46	3.80	0.75	9.74	3.71	1.75	3.75	11.6
² Pentacene	278	2.228	1.35		4.95		5.50		6.18		23.5	
² PhPh	328	1.074	1.07	1.02	0.87	1.54	0.18	1.22	2.36	1.22	0.32	1.56
² TBN	328	1.095	1.09	0.93	1.34	5.22	0.22	9.94	4.55	2.56	0.50	17.2
² Coronene	300	1.002	1.00		3.97		1.79		6.06		5.44	
² Bengo[ghi]perylene	276	1.124	1.35	0.91	1.88	1.11	2.10	1.20	4.09	0.93	2.21	1.29
² Indeno[1,2,3-cd]pyrene	276	1.388	1.23		2.10		2.52		3.83		2.85	

2

^a Mobile phase: methanol/water (90:10) for PAHs (1) and ethanol (100%) for PAHs (2) and for stationary phases (x). Mobile phase: methanol/water (55/45) for PAHs (1-2) for stationary phase (y). Column temperature: 20 °C. Flow rate: 1.00 mL/min.

observed that the retention of isomeric PAHs (i.e., phenanthrene and anthracene, triphenylene, benz[*a*]anthracene, chrysene, and naphthacene, or benzo[*e*]pyrene, perylene, and benzo[*a*]pyrene, or dibenzo[*a,c*]anthracene, dibenz[*a,h*]anthracene, and pentacene) on Sil-DSG increases with increasing L/B ratio as a similar phenomenon was observed for other columns with lower selectivity. The elution of PAHs isomers in Sil-DSG and Sil-ODA₂₅ followed the retention ordered in polymeric C₁₈ phase while Sil-DBG followed the monomeric C₁₈ one. The elution of indeno[1,2,3-*cd*]pyrene followed benzo[*ghi*]perylene in monomeric C₁₈ column, and the lack of resolution of acenaphthene and fluorene, and dibenzo[*a,h*]anthracene and dibenzo[*a,c*]anthracene are also a common phenomenon. A similar pattern was also observed for Sil-DBG. While the elution of benzo[*ghi*]perylene followed by indeno[1,2,3-*cd*]pyrene occurred in Sil-DSG and Sil-ODA₂₅ as well as polymeric C₁₈, better resolutions were also obtained for acenaphthene and fluorene, dibenzo[*a,h*]anthracene, and dibenzo[*a,c*]anthracene by Sil-DSG than all other stationary phases. The chromatograms for four-ring PAHs by different phases are shown in Figure 5. It is observed that Sil-DSG ($\alpha_{\text{Naphthacene/Chrysene}} = 2.3$) can recognize molecular linearity or slenderness better than both Sil-ODA₂₅ ($\alpha_{\text{Naphthacene/Chrysene}} = 1.85$) and polymeric C₁₈ ($\alpha_{\text{Naphthacene/Chrysene}} = 1.4$).

Selectivity for SRM869a Test Mixture. The shape selectivity performance of Sil-DSG and Sil-DBG was also assessed by

SRM869a, the column selectivity test mixture for liquid chromatography.^{64–66} The test was originally developed to facilitate the classification of C₁₈ column in terms of stationary-phase bonding chemistry (i.e., monomeric vs polymeric surface modification) and to evaluate the selectivity for shape-constrained solutes. In recent studies, SRM 869a has also been used to characterize column selectivity for longer alkyl chain length stationary phases.^{24,67} The elution order of the probe compounds is indicative of column selectivity toward a variety of classes of shape-constrained solutes such as PAHs, PCBs, and carotenoids. In general, late elution of BaP relative to TBN indicates enhanced column selectivity toward PAH isomers. Early elution of BaP indicates reduced shape selectivity, and the elution order is typical of most commercial monomeric C₁₈ columns. Figure 6 shows the chromatogram of SRM869a test mixture on Sil-DSG and Sil-DBG phase. It was found that Sil-DSG ($\alpha_{\text{TBN/BaP}} = 0.26$) showed polymer-like retention behavior with extremely enhanced shape selectivity compared to other phases investigated, followed by Sil-ODA₂₅ ($\alpha_{\text{TBN/BaP}} = 0.39$)

(64) Sander, L. C.; Wise, S. A. SRM869, Column Selectivity Test Mixture for Liquid Chromatography (Polycyclic Aromatic Hydrocarbons). Certificate of Analysis. NIST, Gaithersburg, MD, 1990.

(65) Sander, L. C.; Wise, S. A. SRM869, Column Selectivity Test Mixture for Liquid Chromatography (Polycyclic Aromatic Hydrocarbons). Certificate of Analysis. NIST, Gaithersburg, MD, 1998.

(66) Sander, L. C.; Wise, S. A. *LCCG* **1990**, *8*, 378–390.

(67) Sander, L. C.; Pursch, M.; Wise, S. A. *Anal. Chem.* **1999**, *71*, 4821–30.

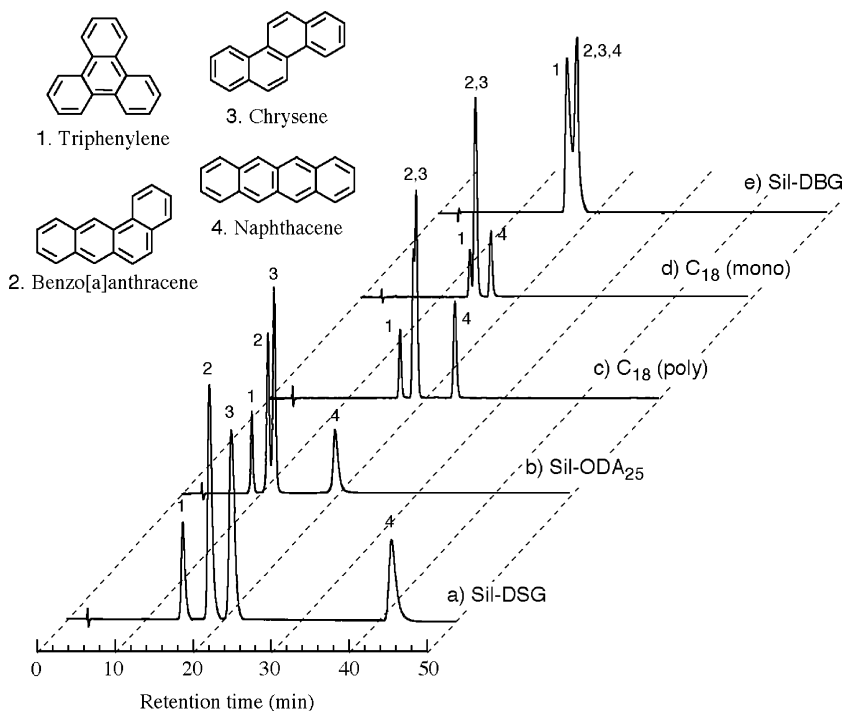


Figure 5. Chromatogram for four-ring PAHs on different columns. Mobile phase: methanol–water (90/10 v/v) for all columns except Sil-DBG as methanol–water (55/45 v/v) used for Sil-DBG at 1.00 mL min^{-1} flow rate. Column temperature: $25 \text{ }^\circ\text{C}$. Detection: UV at 254 nm . Injection volume: $5 \mu\text{L}$.

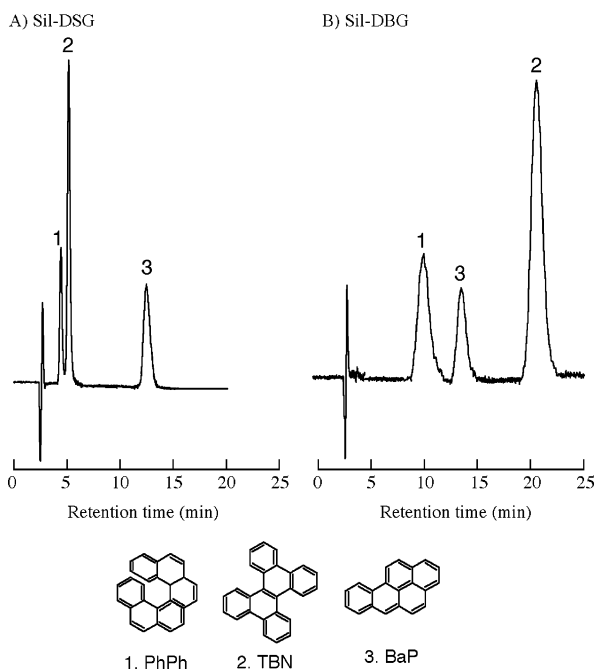


Figure 6. Separation of SRM869a, Column Selectivity Test Mixture for Liquid Chromatography, on (a) Sil-DSG and (b) Sil-DBG columns. Mobile phase: methanol for Sil-DSG and methanol–water (50/50 v/v) for Sil-DBG at 1.00 mL min^{-1} flow rate. Column temperature: $20 \text{ }^\circ\text{C}$. Detection: UV at 254 nm . Injection volume: $5 \mu\text{L}$.

and polymeric C_{18} phases ($\alpha_{\text{TBN/BaP}} = 0.86$). On the other hand, Sil-DBG ($\alpha_{\text{TBN/BaP}} = 1.63$) yielded a monomeric-like ($\alpha_{\text{TBN/BaP}} = 1.64$) retention for SRM 869a. Further examination of selectivity was carried out using phenanthrene and anthracene as test solutes. Similar solute pairs have been used previously to assess resolution obtainable on other columns employed for PAH separations.⁶⁸ The relatively higher ($\alpha_{\text{Anthracene/Phenanthrene}} = 1.38$)

selectivity obtained by Sil-DSG column is related to the homogeneous distribution of DSG molecules on the silica surface. One of the most difficult PAHs pairs to separate with nonshape selective phase is benzo[*a*]anthracene/chrysene. But this critical pair can be separated by Sil-DSG ($\alpha_{\text{Chrysene/Benzo[}a\text{]Anthracene}} = 1.23$) while polymeric C_{18} showed less selectivity for this set of PAHs ($\alpha_{\text{Chrysene/Benzo[}a\text{]Anthracene}} = 1.03$).

Separation Mechanism for Lipid Grafted Noncrystalline Stationary Phase. Generally, the molecular shape selectivity in C_{18} phase increases with increasing carbon loading; i.e., higher alkyl chain density exhibits higher molecular shape selectivity.^{57,69–71} However, Sil-DSG showed extremely enhanced selectivity toward shape-selective compounds compared to other columns investigated regardless of the fact that Sil-DSG had a lower surface coverage and lower alkyl chain density than polymeric C_{18} and Sil-ODA₂₅. It was also observed that monomeric C_{18} phase showed higher alkyl chain density than Sil-DBG but showed lower planarity recognition for planar and nonplanar PAHs. The unusually enhanced molecular shape selectivity yielded by Sil-DSG cannot be explained by common phenomena alone, as shape selectivity is high with higher bonding density and alkyl phase chain length.^{20–24} To explain the unique selectivity of the Sil-DSG phase, we applied a multiple carbonyl π –benzene π interaction mechanism. We have reported previously that carbonyl groups in Sil-ODA_{*n*} are polarized to δ^+ (carbon) and δ^- (oxygen).⁵³ These polarized atoms can work as an electrostatic source of π – π interaction in which carbon atoms act as electron donors and

(68) Pursch, M.; Sander, L. C.; Egelhaaf, H. J.; Raitza, M.; Wise, S. A.; Oelkrug, D.; Albert, K. *J. Am. Chem. Soc.* **1999**, *121*, 3201–13.

(69) Sander, L. C.; Parris, R. M.; Wise, S. A. *Anal. Chem.* **1991**, *63*, 2589.

(70) Wise, S. A.; Sander, L. C.; May, W. E. *J. Chromatogr., A* **1993**, *642*, 329.

(71) Sander, L. C.; Wise, S. A. *Retention and Selectivity Studies in HPLC*; Elsevier: Amsterdam, 1994; p 337.

Table 4. Effect of Addition of Acetone to the Mobile Phase on Planarity and Linearity Selectivity of PAHs by Different Phases^a

	alkyl chain density ($\mu\text{mol}/\text{m}^2$)	$\alpha_{\text{TBN/BaP}}$	$\alpha_{\text{naphthalene/chrysene}}$		$\alpha_{\text{triphenylene lo-terphenyl}}$	
			MeOH/H ₂ O (90/10)	MeOH/acetone/H ₂ O (70/20/10)	MeOH/H ₂ O (90/10)	MeOH/acetone/H ₂ O (70/20/10)
C ₁₈ (mon)	1.72	1.63	1.20	1.20	1.50	1.50
C ₁₈ (polym)	3.40	0.86	1.50	1.50	3.00	3.00
Sil-ODA ₂₅	2.63	0.39	2.02	1.91	5.63	4.75
Sil-DBG	1.41	1.64	1.13	1.02	2.70	2.15
Sil-DSG	2.13	0.26	2.42	2.31	6.37	4.92

^a Column temperature: 10 °C. Flow rate: 1.00 mL/min.

interact with π electrons containing guest molecules. The carbonyl groups in stationary phases interact with aromatic elutes through π - π interactions that are stronger (1.87 kcal mol⁻¹ in HCHO-benzene) than those of both CH- π (0.57 kcal mol⁻¹ in CH₄-benzene)⁵³ and benzene π -benzene π (0.49 kcal mol⁻¹ in the plane-to-plane stacking), and the aligned carbonyl groups in Sil-ODA_n are effective for enhancing higher selectivity toward PAHs. Based on that idea, we have clarified those carbonyl groups in the lipid main chain work as a π -electron interaction source for Sil-DSG and Sil-DBG as these contained three carbonyl groups in the glutamide moiety. We have already described that the lipid DSG can aggregate by self-assembly in various organic solvents while DBG cannot aggregate. The electrostatic carbonyl- π and benzene- π interactions worked more effectively in Sil-DSG than Sil-DBG. The carbonyl groups in Sil-DSG form a two-dimensionally condensed layer by forming hydrogen bonding among the glutamide moieties, which makes the carbonyl groups in an ordered form favorable for multiple π - π interactions with the guest PAH molecules. This phenomenon was also supported by ¹³C CP/MAS NMR spectral results, in which the alkyl chain does not form an ordered trans conformation even at lower temperature unlike the polymeric C₁₈ phase. It is known that higher shape selectivity can be obtained by the polymeric C₁₈ phase and that highly ordered octadecyl chains enhance the selectivity. This also strongly supports our hypothesis of a π - π interaction mechanism. Furthermore, since the separation factor (α) values remained unchanged in Sil-DSG and Sil-DBG after 0.01% trifluoroacetic acid (TFA) was added into the mobile phase, the selectivity is independent of the remaining amine groups on the silica. These facts strongly suggest that the higher selectivity of Sil-DSG were brought about through the carbonyl groups of the glutamide moieties. In support of this hypothesis, when we added acetone (an inhibitor for π - π interactions) to the mobile phase, the selectivity for Sil-DBG and Sil-DSG was found to decrease for PAHs (as shown in Table 4). A similar reduction was observed for Sil-ODA₂₅, but no change of selectivity was found for either monomeric or polymeric C₁₈ phases. These results also support our hypothesis that carbonyl groups present in Sil-DSG and Sil-DBG play a significant role in the separation mechanism for these special type stationary phases.

Temperature Dependencies on Selectivity. In general, it has been assumed that the effect of temperature is small and that selectivity decreases with increasing temperature. Recently, however, attention has been paid to the use of temperature as a secondary variable after eluent composition to optimize

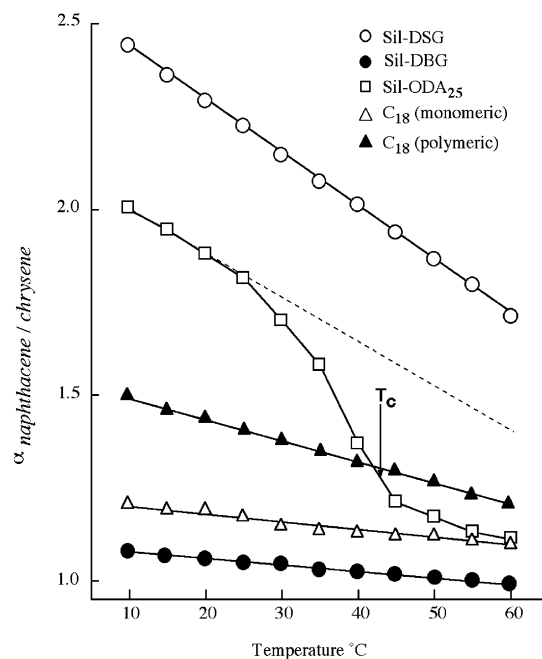


Figure 7. Temperature dependencies on the selectivity of naphthalene and chrysene on different stationary phases (other conditions as described in Figure 5).

separations,⁷²⁻⁷⁴ and column temperature has been shown to have a strong influence on shape selectivity in LC.^{75,76} To understand the temperature dependencies on selectivity of Sil-DSG, Sil-DBG, and Sil-ODA₂₅, the separation factors in temperatures ranging from 10 to 60 °C were examined using naphthalene and chrysene as elutes, and the results are shown in Figure 7. These two PAHs have the same number of carbon atoms and π electrons but different molecular shapes (L/B ratio). Figure 7 shows that the effect of temperature on the selectivity is very low for monomeric C₁₈ ($\alpha = 1.2$ –1.1) as well as for polymeric C₁₈ ($\alpha = 1.5$ –1.2). Sil-ODA₂₅ showed remarkable temperature dependence with high selectivity, especially at a low temperature ($\alpha = 2.1$ at 10 °C) and a distinct bending is attributed to the phase transition between ordered and disordered state of the ODA₂₅ moiety. Similar bending

(72) Snyder, L. R. *J. Chromatogr., B* **1997**, *689*, 105–115.

(73) Zhu, P. L.; Dolan, J. W.; Snyder, L. R. *J. Chromatogr., A* **1996**, *756*, 41–50.

(74) Wolcott, R. G.; Dolan, J. W.; Snyder, L. R.; Bakalyer, S. R.; Arnold, M. A.; Nichlos, J. A. *J. Chromatogr., A* **2000**, *869*, 211–230.

(75) Knox, J. H.; Vasvari, G. *J. Chromatogr.* **1973**, *83*, 181.

(76) Claudy, P.; Letoffe, C.; Gaget, C.; Morel, D.; Sperinet, J. *J. Chromatogr.* **1985**, *329*, 331.

Table 5. Separation Factors (α) of Geometrical Isomers for Various Stationary Phases^a

	<i>trans</i> -/ <i>cis</i> -stilbene	<i>m</i> -/ <i>o</i> -terphenyl	<i>p</i> -/ <i>m</i> -terphenyl	<i>m</i> -/ <i>o</i> -phenyltoluene	<i>p</i> -/ <i>m</i> -phenyltoluene	γ -/ α -terpinene
C ₁₈ (mon)	1.08	1.52	1.03	1.10	1.00	1.02
C ₁₈ (polym)	1.33	1.70	1.26	1.23	1.09	1.10
Sil-ODA ₂₅	2.15	1.86	1.90	1.34	1.24	1.10
Sil-DBG	1.44	1.75	1.05	1.20	1.04	1.07
Sil-DSG	3.04	1.95	4.29	1.35	1.35	1.12

^a Mobile phase: methanol/water 70/30. Column temperature: 20 °C. Flow rate: 1.00 mL/min.

was observed in *trans*-stilbene, *cis*-stilbene, triphenylene, and *o*-terphenyl.⁷⁷ DSC measurement of Sil-ODA₂₅ showed an endothermic peak in the range of 30–47 °C, with a peak top at 42 °C in a methanol–water (45:55) suspension. This temperature range is close to the bending temperature in Figure 7. Therefore, the selectivity enhancement of Sil-ODA₂₅ was brought about by ordering of the organic phase. On the other hand, Sil-DSG, Sil-DBG, and C₁₈ phase did not show any phase transition in the temperature ranges from 10 to 60 °C, and no such bending or sudden decrease of selectivity was observed for these phases. The thermal effects on the elution of the analytes can be explained in two ways. First, at higher column temperatures, the thermal mobility of the bonded-phase chain (Sil-DSG) becomes greatly enhanced like C₁₈, and this reduces the hydrophobic interaction as well as π – π interaction between the stationary phases and the analytes, resulting in increased distribution of the analytes into the mobile phase. Second, as the temperature of the mobile phase is increased, the solubility of the analytes is also increased, which facilitates the distribution of analytes into the mobile phase, leading to reduced retention times.

Selectivity toward Geometrical Isomers. A series of phenyl-substituted isomers were used to examine the isomeric selectivity of Sil-DSG and Sil-DBG. The separation factors of different geometrical isomer sets are shown in Table 5. As shown in the table, Sil-DSG showed enormously higher selectivity for geometrical isomers, especially for the long narrow molecules (para and trans isomers). The selectivity of geometrical isomers on Sil-ODA_n is enhanced by the carbonyl– π interaction, and this is more pronounced for trans and para isomers.⁷⁴ Multiple interac-

tions are an advantage in recognition of isomers and are especially effective in case of planar-to-planar and rigid-to-rigid structures.⁷⁸

CONCLUSION

In this work, we have discussed the new application of L-glutamide derivatives in separation science, especially as stationary phases in high-performance liquid chromatography. The alkyl moiety in Sil-DSG exists in a solid and noncrystalline state after immobilization on to the silica surface and no conformational change of alkyl chain occurs. Spectroscopic results of Sil-DSG indicated that the carbonyl groups are rigidly immobilized on the silica surface and might form condensing layers. Inter- or intramolecular hydrogen bonding most likely promotes this assembly and can be a driving force for multiple π – π interactions. The enhancement of selectivity in this phase is due to multiple π – π interactions, and it was endorsed by orientating the carbonyl groups of the glutamide moieties that assembled themselves in DSG. In Sil-ODA_n, the carbonyl groups can be oriented by forming a highly ordered structure of the side chains, and a thermally induced disordered-to-ordered phase transition was also observed. On the other hand, Sil-DSG and Sil-DBG did not show any phase transition behavior in DSC, suspension-state ¹H NMR, and also in HPLC measurement. This idea of π – π interaction between the stationary phases might be helpful for further development of stationary phases in liquid chromatographic science. Finally, from our detailed investigation, we hope this novel HPLC packing material (Sil-DSG) can play a significant role for the separation of PAHs and aromatic positional isomers.

(77) Ihara, H.; Nagaoka, S.; Tanaka, H.; Sakaki, S.; Hirayama, C. *J. Liq. Chromatogr.* **1996**, *19*, 2967.

(78) Takafuji, M.; Dong, W.; Goto, Y.; Sakurai, T.; Nagaoka, S.; Ihara, H. *Polym. J.* **2002**, *34*, 437–442.

Received for review May 17, 2005. Accepted August 14, 2005.

AC050851V